Inventory of Supplements

- **Figure S1: Chart summarizing of the evidence used to assign identities to each cell type, related to Figures 2 and 3.** Cell lineage up to the 16-cell stage. Each cell type is color-coded by the types of evidence that contributed to the identification of the transcriptomes of that cell type.
- **Figure S2: Fine details for assigning cell-identities to each transcriptome, related to Figures 2 and 3.** All heatmaps and PCAs referred to "Assigning Cell Identities to Each Transcriptome" section of Extended Experimental Procedures that are not included in Figures 2 and 3.
- **Figure S3: Comparisons to related existing datasets, related to Figure 4.** Comparisons and AB and P1 transcriptome between present study and two previous ones (Hashimshony et al. 2012 and Osborne Nishimura 2015). (B) Comparisons between present study and whole-embryo micro-array dataset from Baugh et al. 2005.
- **Figure S4: RNAi targeting synexpressed paralogous genes results in embryonic lethality, related to Figure 6.** Embryonic lethality of RNAi targeting either T24E12.1 or T24E12.13 independently in N2 worms. (B) Embryonic lethality of co-injection of dsRNA targeting pairs of synexpresed paralogous genes in *rrf-3* worms.
- **Table S1: Summary of all 219 samples sequenced, related to Experimental Procedures.** Sample name, NCBI GEO accession number, and experimental details about each sample sequenced.
- **Table S2: Normalized expression levels for all genes in all samples, related to Figure 1.** Reads per kilobase per million reads of each transcript for all 219 samples sequenced.
- **Table S3: 295 sets of paralogous, synexpressed genes, related to Figure 6.** Sets of 2-5 genes with high sequence similarity were grouped and the average correlation coefficient of mRNA expression patterns for each group was calculated.
- **Supplementary Figure Legends**
- **Extended Experimental Procedures**
- **Supplementary References**

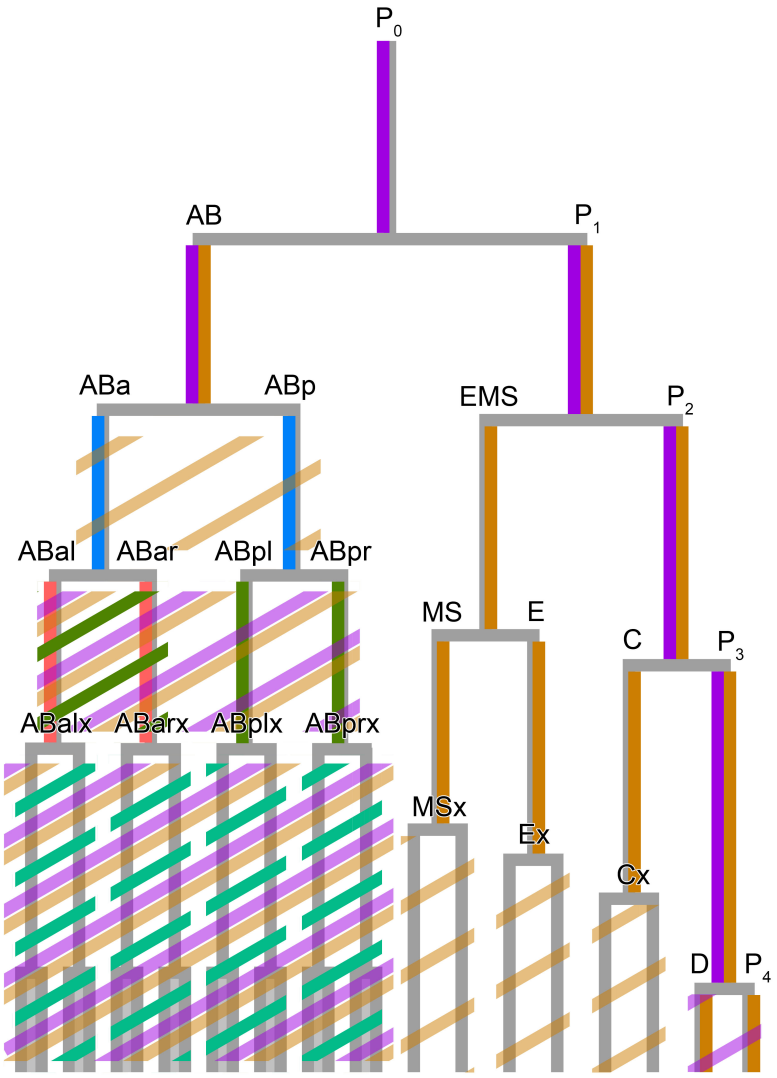

ID known before sequencing (either by cell size or division timing)

PCA / candidate genes

Hand sorted with notch target genes (*hlh-27* and *ref-1*)

PCA with 7 notch target genes

PCA with genes whose transcripts are

PCA with genes differentially enriched between *tbx-38*$^{+}$ and *tbx-38*$^{-}$ cells

Identified to a single-cell resolution

Identified to a multi-cell resolution

"-x" both the anterior ("-a") and posterior ("-p") siblings

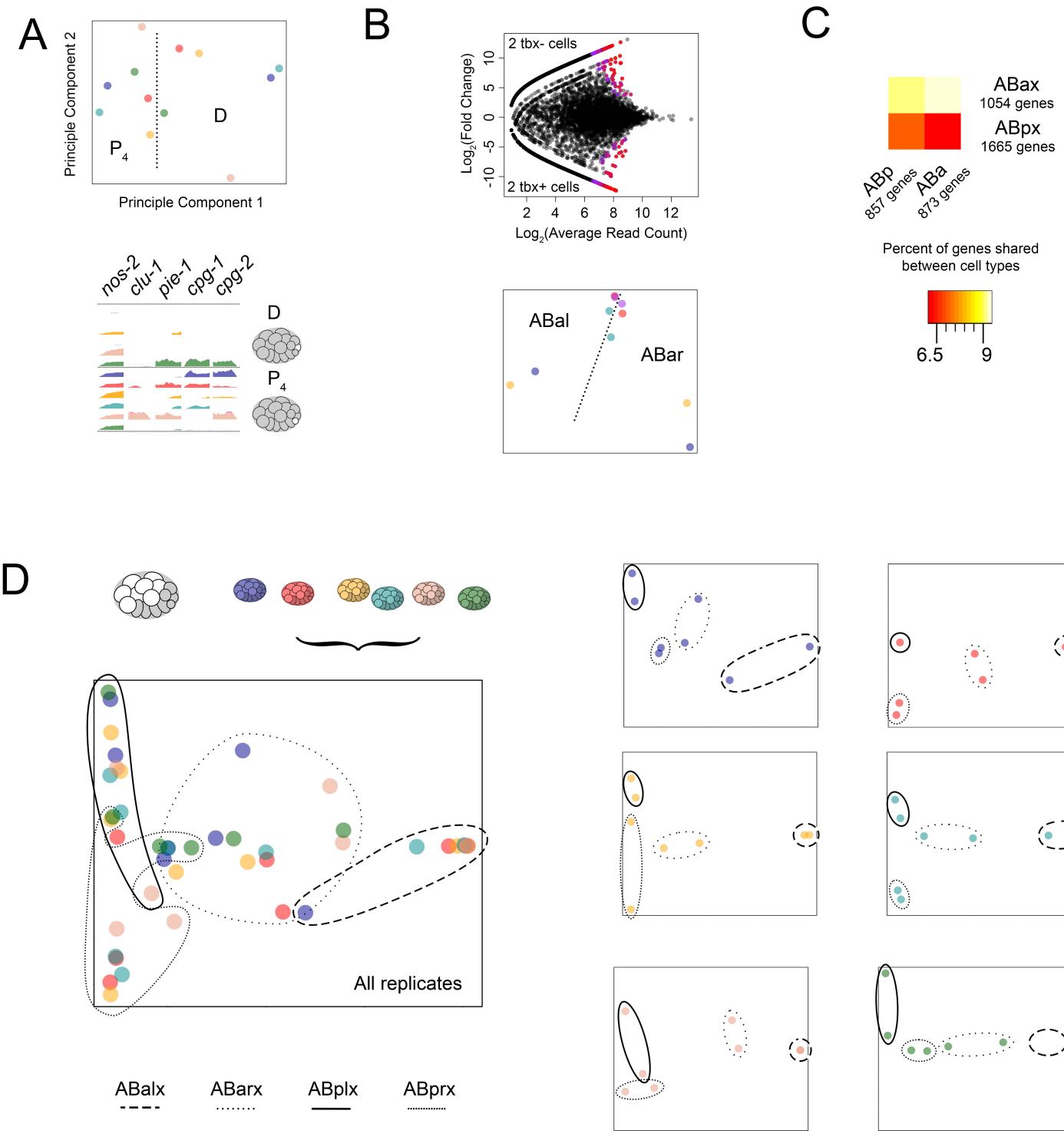
A
Principle Component 2
Principle Component 1
D
P4
nos-2
clu-1
pie-1
cpg-1
cpg-2
D
P4
B
2 tbx- cells
2 tbx+ cells
Log2(Fold Change)
Log2(Average Read Count)
ABal
ABar
C
ABax
1054 genes
ABpx
1665 genes
ABp
857 genes
ABa
873 genes
Percent of genes shared
between cell types
6.5
9
D
All replicates
ABalx
ABarx
ABplx
ABprx

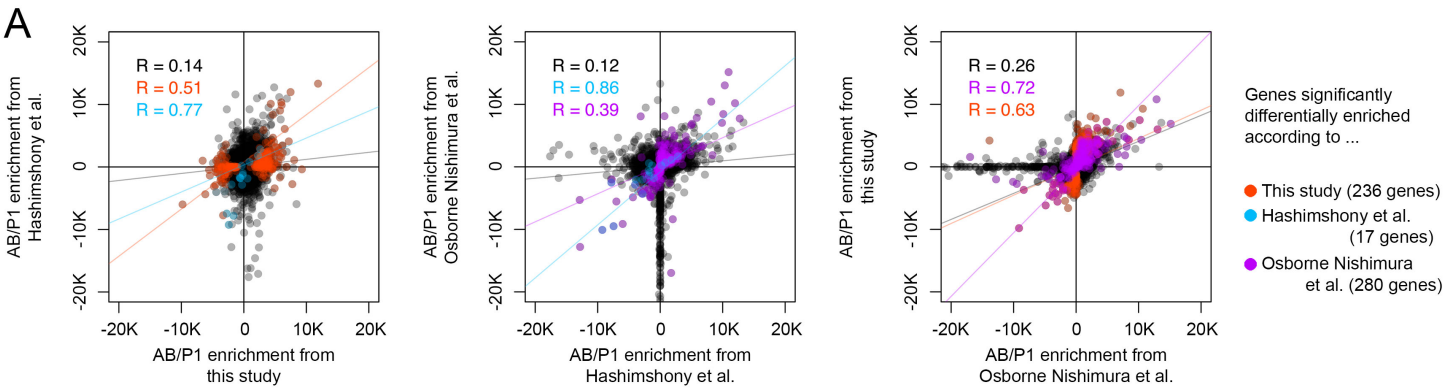
A
AB/P1 enrichment from Hashimshony et al.
AB/P1 enrichment from this study
R = 0.14
R = 0.51
R = 0.77
AB/P1 enrichment from Osborne Nishimura et al.
AB/P1 enrichment from Hashimshony et al.
R = 0.12
R = 0.86
R = 0.39
AB/P1 enrichment from this study
AB/P1 enrichment from Osborne Nishimura et al.
R = 0.26
R = 0.72
R = 0.63
-20K
-10K
0
10K
20K
Genes significantly differentially enriched according to ...
This study (236 genes)
Hashimshony et al. (17 genes)
Osborne Nishimura et al. (280 genes)

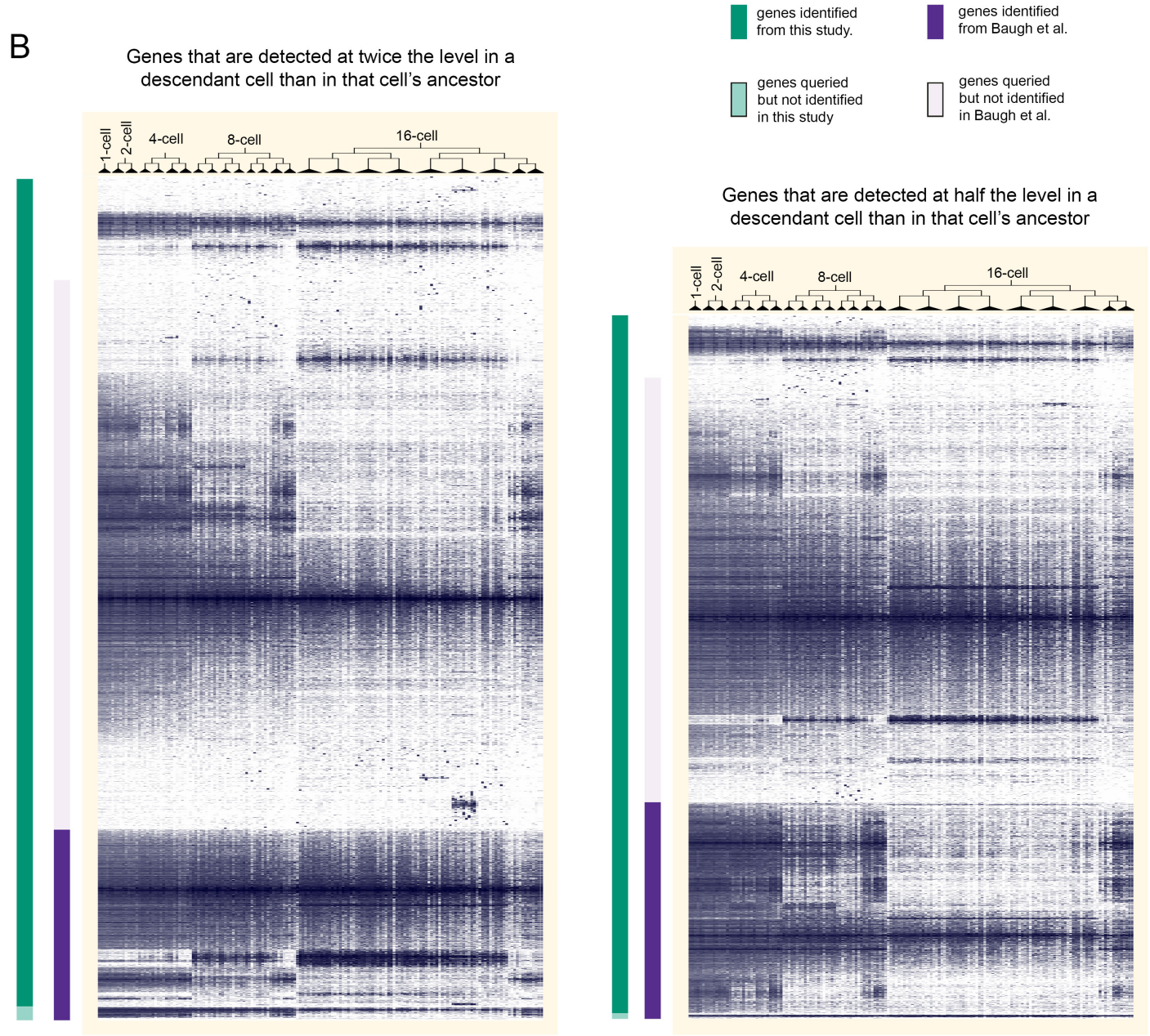
B
genes identified from this study.
genes identified from Baugh et al.
genes queried but not identified in this study
genes queried but not identified in Baugh et al.
Genes that are detected at twice the level in a descendant cell than in that cell's ancestor
1-cell
2-cell
4-cell
8-cell
16-cell
Genes that are detected at half the level in a descendant cell than in that cell's ancestor

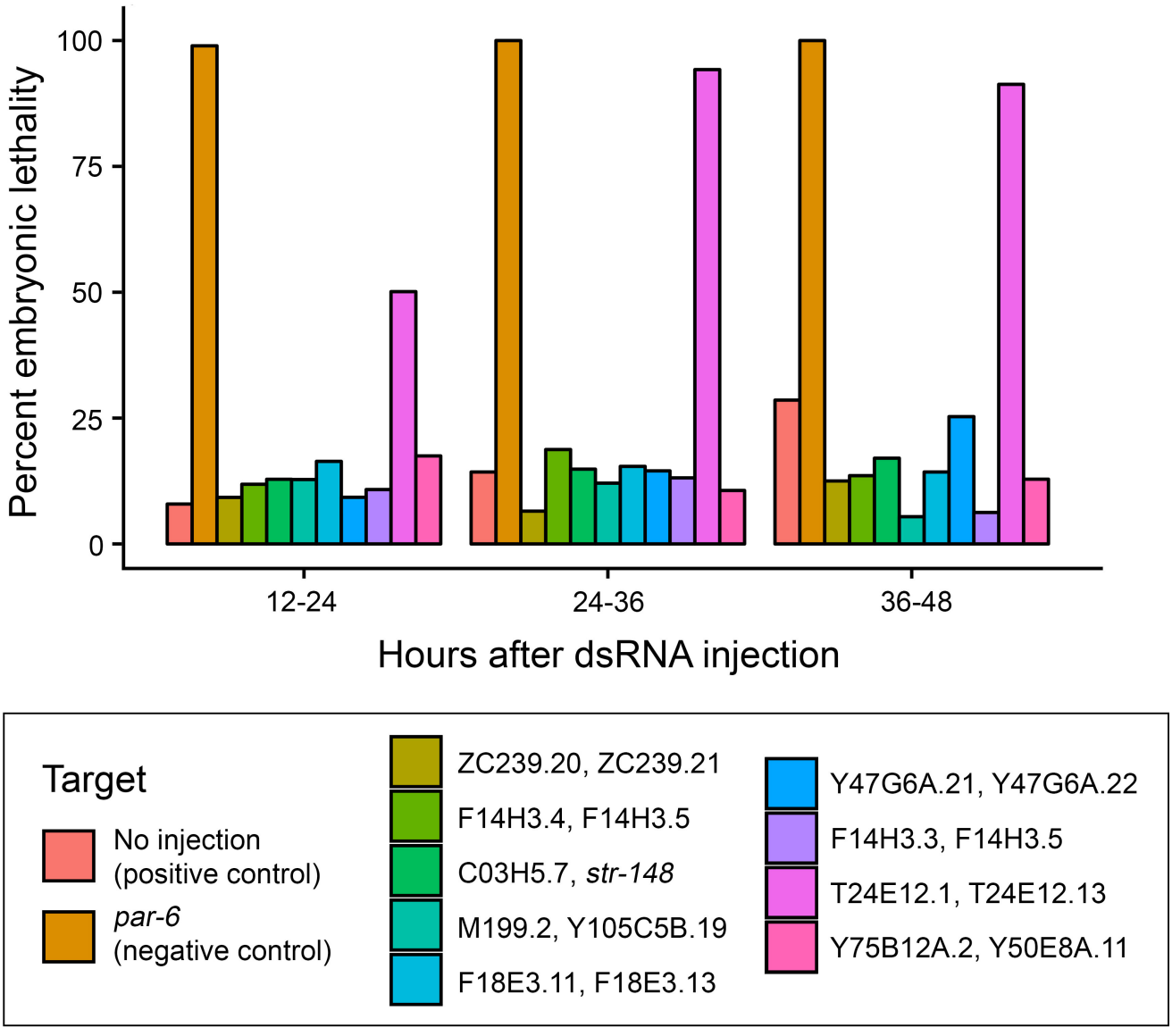
Percent embryonic lethality
100
75
50
25
0
12-24
24-36
36-48
Hours after dsRNA injection
Target
No injection
(positive control)
par-6
(negative control)
ZC239.20, ZC239.21
F14H3.4, F14H3.5
C03H5.7, str-148
M199.2, Y105C5B.19
F18E3.11, F18E3.13
Y47G6A.21, Y47G6A.22
F14H3.3, F14H3.5
T24E12.1, T24E12.13
Y75B12A.2, Y50E8A.11

Supplementary Figure Legends

Figure S1: Chart summarizing of the evidence used to assign identities to each cell type, related to Figures 2 and 3

Cell lineage up to the 16-cell stage. Each cell type is color-coded by the types of evidence that contributed to the identification of the transcriptomes of that cell type. Detailed description of each type of evidence in Extended Experimental Procedures.

Figure S2: Fine details for assigning cell-identities to each transcriptome (Detailed in Extended Methods), related to Figures 2 and 3

(A) PCA of transcriptomes from the D&P_4 cluster in Figure 2N (top). Genome browser tracks for the last exon of several genes with germline-enriched transcripts (bottom).

(B) MA plot of differential expression analysis between the two *tbx-38* enriched ABax cells (of the 8-cell stage), and their non *tbx-38* enriched sister cells (top). PCA performed on all ABax cells using only expression data from genes found to be differentially expressed in the MA plot (bottom).

(C) Heatmap of the percentage of overlap between ABax-enriched genes or ABpx-enriched genes, and genes enriched in either of the two ABx cell types (ABa or ABp). These data were used to provide tentative assignments to ABa versus ABp cells. Based on this plot, we assigned the identity of ABa to the group of cells that shares a larger percentage of genes with ABal and ABar, and we assigned the identity of ABp to the group of cells that shares a larger percentage of genes with ABpl and ABpr.

(D) PCA performed on all ABxxx transcriptomes of the 16-cell stage using data from only 7 notch target genes (*hlh-25*, *hlh-26*, *hlh-27*, *hlh-29*, *tbx-38*, *tbx-39* and *ref-1*). Circles of varying line types delineate the cell identity groupings. The same plot is shown to the right, split out into contributing embryos.

Figure S3: Comparisons to related existing datasets, related to Figure 4

(A) Correlations of differential enrichment indexes for each gene according to three independent studies (present study, Hashimshony et al. 2012, Osborne Nishimura et al. 2015). Black dots represent all genes. Colored dots represent the genes that are significantly differentially enriched

between AB and P_1, as reported by this study (red points, p-value < .05 after FDR adjustment using EdgeR package), Hashimshony et al. 2015 (blue points, p < .05, after FDR adjustment) or Osborne Nishimura et al. 2015 (purple points, p < .1 after FDR adjustment, using DESeq package). The enrichment index of each transcript, for a given dataset, is determined by multiplying the log fold change for that transcript between AB and P1 by the average abundance raised to the fourth power.
(B) Heatmap of transcript abundance levels in all quality-filtered samples (x-axis) for genes (y-axis) whose transcript abundances were found to increase (left) or decrease (right) over time in either this study or Baugh et al. 2005. Color key for heatmap is shown in Figure 4B.

Figure S4: RNAi targeting synexpressed paralogous genes results in embryonic lethality, related to Figure 6

(A) Embryonic lethality of RNAi targeting either T24E12.1 or T24E12.13 independently in N2 worms. Results of co-injection are shown in Figure 6G.
(B) Embryonic lethality of co-injection of dsRNA targeting pairs of synexpresed paralogous genes in *rrf-3* worms.

Table S1: Summary of all 219 samples sequenced

Data includes sample name (unique identifier, cell type, embryo stage, and replicate number), NCBI GEO accession number, whether the sample was used, estimated picograms of RNA detected in sample, number of unique reads per sample, and number of mRNA species detected over 25 RPKM.

Table S2: Normalized expression levels for all genes in all samples

Reads per kilobase per million reads of each transcript for all 219 samples sequenced. See Table S1 for details on each sample.

Table S3: 295 sets of paralogous, synexpressed genes.

Sets of 2-5 genes with high sequence similarity were grouped (Experimental Procedures) and the average correlation coefficient of mRNA expression patterns for each group was calculated. Of

these sets of genes, 295 had an average expression pattern correlation of above 0.25 (pink box in Figure 6A). All 295 sets and their average correlation coefficients are described here.

Extended Experimental Procedures

Embryo Dissections

For each single embryo dissected, eggshells were weakened with 10% bleach in Egg Buffer for 3 minutes followed by a 3-5 minute incubation in 20 units/mL chitinase and 10 mg/mL chymotrypsin in Egg Buffer. Cells were manually teased apart by aspiration in Shelton's media. Cells used for 16-cell samples were separated from each other at the 12 cell stage, so that the final cell divisions could be observed immediately before embryos were collected into 16 tubes at the 24-cell stage (all 16 AB cells were collected as 8 pairs of sister cells). All cells from an embryo were simultaneously flash frozen in liquid nitrogen and stored at -80°. Only complete sets of cells were processed for 1-cell through 8-cell samples. For 16-cell samples, sets of cells were processed if at least 14 cells remained intact. Of the 16-cell replicates that passed quality filtration, two replicates had all 16 samples, three replicates were missing one descendant of P_1, and one replicate was missing 2 descendants of AB. All replicates of any given stage were collected on independent days and processed on independent days, with the exception of the first and second 1-cell stage replicates.

RNA preparation, sequencing and RPKM generation

The 3' SMART CDS Primer IIA contains a poly-T region followed by a lock-docking –VN degenerate region, which reduces the possibility of preferentially capturing transcripts with the longest polyadenylated stretches. ERCC RNA spike-in controls were added at a 1:2,000,000 dilution, with the exception of the first replicate of the 4-cell stage, which was diluted 1:500,000. All libraries were sequenced on a Hi-Seq 2500 Illumina machine, for 50 cycles from a single end. Identical reads were collapsed using fastx_collapser (FASTX Toolkit 0.0.13.2; Gordon & Hannon 2010) and aligned to the ce10 genome using Tophat2 (2.0.11; Kim et al. 2013). Count files were generated using HTseq-count (HTSeq 0.5.3p3; Anders et al. 2014) and a WBcel235.78.gtf reference file (ftp.ensemble.org).

Transcriptome analyses

Analyses were performed in R. All scripts and functions are available at https://github.com/tintori/transcriptional-lineage. In all analyses, genes were only considered expressed if their transcripts were detected above 25 RPKM.

RNAi

Double stranded RNAs were made using primers defined below. dsRNAs were generated with Promega's T7 Ribomax Express RNAi kit, according to manufacturers instructions. After injection, worms were moved to fresh plates every 12 hours, and plates were assayed 24 hours later for number of larval offspring and unhatched eggs.

Primers for dsRNA

Target	Forward Primer	Reverse Primer
par-6	ATGTCCTACAACGGCTCC	TCAGTCCTCTCCACTGTCC
ZC239.21	ATGTCCTTCTCATCCTGCT	TTAAAGCATTTGCATCTTCATCG
ZC239.20	AATCTCAACCTCCTCAAAATGTC	AGTAATTCATTTATTAAGAATAAAAGTTGAAAATTAAT
F14H3.5	ATGAGTGAACCGTCAAATAATTCCGAG	CCGCCAAATGTTTATGAAATTCAAAATTAAATAAACTC
F14H3.4	ATCTTTCACCAACAAAATGAGTG	CTTATCTTTAAATTTTTATAAAATTCAAAATTAACTC
str-148	ATGTCAAATACTGTTGAGAAACAGTTG	TCAGTGTCAATACAATTTTTCAAAAATAAATTAACT
C03H5.7	ATTCCTCATTTGAAAATGCCCG	CCATTATTTTATTTATTTTCAGAAAATTTTTCAAGTC
Y105C5B.19	ATGTCCCGCCGAGCT	GCTGGAAAAACTTTTATATAGACAGCTGAAATG
M199.2	AGATGCCAGGCCCAACTCC	TTTCATTTGGTCAAATGTGTATCCAATTCAATGAAG
F18E3.13	AATCAACCAATTCTCACATCGAATCGT	TTTTTGAGAATGAATTATTTTTATTGAATGACTTCATGTAC
F18E3.11	TAACCTATTCTCACTTCGAATCGT	AAATAGTGAATTAATTTATTGAGATCAAATCATG
Y47G6A.22	GTCAACCATGCCCGTC	AAAAATACATGTATCTCTCTATTTATTACATG
Y47G6A.21	AGTATCCGAAAATGCCAGTCGC	TTGGTACAAATTTACTTCATTCTCAATTTTCAAAAC
F14H3.5	ATGAGTGAACCGTCAAATAATTC	CCGCCAAATGTTTATGAAATTC
F14H3.3	AGTGACCCGACGCAAAA	TACAGATGTTTGTAAATTCATGATCAAGTTAC
T24E12.13	GTTTCAGATCATGCCAGATATG	TCAATACATCTCCATTATTTCCTG
T24E12.1	AGATTTAAAGGCTGAAGGAAATG	AATTCAATTTATTGATAACAAATATGAGATATG

Y75B12A.2	ATGTGCTCTTATTCTCTTG CTCCGGC	TCAAAAAAGGCTATGTGGCTCTGCGG
Y50E8A.11	ATGGTTTCTGCCACTGGAC ATCTTCG	AATTTATTCATTTAGTTATATTTTTT

Single molecule fluorescent in situ hybridization

Stellaris smFISH fluorescent probe sets (Biosearch) were generated to target transcripts. Gravid worms were bleached for embryos, resuspended in -20°C methanol, freeze cracked in liquid nitrogen, and fixed at -20°C for 24–48 hours (as in Shaffer et al. 2013). Embryos were equilibrated in WB1 (100 mg/ml dextran sulfate, 10% formamide, 2 x SSC), hybridized in hybridization buffer (100 mg/ml dextran sulfate, 1 mg/ml *E. coli* tRNA, 2 mM vanadyl ribonucleoside complex, 0.2 mg/ml BSA, 10% formamide) containing 50 picomoles of each primer set (Ji & van Oudenaarden 2012). Hybridization at 30°C overnight was followed by two 10 minute WB1 washes and one 10 minutes WB1/DAPI staining at 30°C. This was followed by three 2 x SSC washes at room temperature. Embryos were mounted as described by Ji & van Oudenaarden 2012, using SlowFade (Life Technologies) to prevent photobleaching. smFISH images were acquired using a Photometrics Cool Snap HQ2 camera on a DeltaVision-modified inverted microscope (IX71; Olympus), with a UPlanSApo 100 x (1.40 NA) objective and SoftWorx software (Applied Precision) using fixed exposure and acquisition conditions (0.3 μm z-stacks, up to three wavelengths using AlexaFluor emission filters). Images were deconvolved using DeltaVision deconvolution.

Assigning Cell Identities to Each Transcriptome

Identities known before sequencing (purple in Figure S1)

Certain cell identities were known during collection based on visible features. At the 1-cell stage, there is only one cell (P_0). At the 2-, 4- and 8-cell stages, the P_1, P_2 and P_3 cells respectively are notably smaller than the others, and at the 16-cell stage the P_4 and D cells are both smaller than the others. By the 8- and 16-cell stages cell divisions remain quick and synchronous in the anterior cells, and become asynchronous in the posterior cells. By isolating cells right before the

final cell division (at either 6 cells or 15 cells, respectively), cells from the anterior were distinguished from cells of the posterior, based on the timing of the final divisions. Because of the asynchrony in cell division, there is not 16-cell stage *per se*; by the time the posterior half of the embryo consists of 8 cells, the anterior half of the embryo has just divided from 8 to 16 cells. We collected those 8 pairs of anterior sisters as 8 samples. Once identified, we refer to them by the 8 names of their parent cells. For example, ABalaa and ABalap, having just divided from each other, were collected together as one sample, which we refer to as ABala. As a result, whenever we refer to the 16-cell stage we are actually referring to the 24-cell stage collected in 16 samples; 8 samples are single (posterior) cells, and 8 samples are pairs of newborn sister (anterior) cells. This is illustrated by the end of the cell lineage tree in Figure 1A.

Clustering transcriptomes by multi-gene approach and identifying clusters using candidate genes (orange in Figure S1)

For each stage we used an algorithm to filter for a set of informative genes, and then used that set of genes in a Principle Component Analysis (PCA) to sort transcriptomes into clusters of replicates. In this way we matched transcriptomes by similar (though unknown) cell type. The algorithm for gene selection identifies the 100 most cell-specific genes for each transcriptome of a given stage. It then selects only genes that show up in these lists for at least three distinct embryos. This generates a list of genes that reproducibly describe differences between the cells of that stage. For the 2-cell stage, this algorithm selected a list of 43 genes (Set 1, below), which segregated the transcriptomes into two groups, each group containing a single transcriptome from each embryo (Figure 2B). We examined these transcriptomes for transcripts known to be enriched in AB or P_1, and found that one group of transcriptomes was enriched for *cpg-2* transcripts (known to be P_1 specific), and the other group was enriched for *erm-1* transcripts (known to be AB specific; Osborne Nishimura et al. 2015; Figure 2C). These AB and P_1 identity assignments independently matched our expectations based on the differential sizes AB and P_1 cells noted during sample collection.

At the 4-cell stage, the algorithm selected 150 genes (Set 2, below), which segregated EMS and P_2 cells into distinct groups (Figure 2D). We identified these groups as EMS and P_2 based on their enrichment of *med-2* and *cpg-2* transcripts, respectively (Figure 2G; Maduro et al. 2007). The remaining cells showed an enrichment of *erm-1* mRNA, supporting their identities as

ABa and ABp cells (Figure 2G). To distinguish between these two cell types, we re-ran the gene selection algorithm and PCA on just those remaining ABx cells (40 genes, Set 3, below), which sorted the transcriptomes into two distinct clusters (Figure 2F), but were not able to identify which cluster represented which cell type, as we did not know of candidate genes that could distinguish between them.

We ran the algorithm and PCA on all replicates of the 8-cell stage, and using 453 genes (Set 4, below), identified two groups of cells (Figure 2I). Both of these groups were enriched for genes that are associated with the germ line (Figure 2L), and one cluster was composed of all the cells we knew to be P_3 cells, based on their differential size during sample collection. Based on this evidence, we assigned the identity of P_3 to this cluster, and the identity of C on the cluster positioned between P_3 and the remaining transcriptomes. The algorithm selected a new set of genes (295 genes, Set 5, below) and we performed another PCA with the remaining cells (Figure 2J). In this plot we saw two more distinct groups of transcriptomes segregate. One group showed enrichment for E-specific genes such as *end-3* (Maduro et al. 2005). The other group showed enrichment for MS-specific genes, such as *tbx-35* (Figure 2L; Robertson et al. 2004). We therefore assigned the identities of E and MS to the transcriptomes in each of these groups. There was one replicate not represented in the MS cluster of transcriptomes. We noticed that one of the libraries from the embryo that was missing in the MS cluster has an extremely low yield during sequencing. While that low-quality transcriptome was the only one from that embryo to show expression of MS-specific marker genes, it did not cluster with the other MS cells. This is presumably because the library prep failed, and the artifacts of a low-quality library were preventing this transcriptome from grouping with others in a biologically relevant way. We excluded this transcriptome from further analysis. Further rounds of gene selection and PCA on the remaining cells, all the descendants of AB (169 genes, Set 6, below), did not yield any further distinctions (Figure 2K). These remaining cells were the ones we identified earlier as AB descendants based on their synchronized cell divisions, and they showed enrichment of AB specific genes such as W02F12.3 (Osborne Nishimura et al. 2015), independently supporting our hypothesis that these were AB descendants.

We put all cells from all replicates of the 16-cell stage through our gene selection algorithm, which selected 508 genes (Set 7, below). When we performed PCA with these genes on all 16-cell transcriptomes, two groups segregated out, each containing two transcriptomes

from each embryo (Figure 2N). One such group of two transcriptomes per embryo showed enrichment for transcripts of germ cell specific genes, such as *cpg-2* (Figure 2Q), suggesting P_4 and D fates, and one group expressed transcripts of the gut precursor gene *end-1*, suggesting Ea and Ep fates (Maduro et al. 2007; Zhu et al. 1997). As shown in Figure S2A, we were able to further split the D/P_4 group into two separate groups using 73 informative genes (Set 8, below). We examined expression levels of a panel of germ cell specific genes (*nos-2*, *clu-1*, *pie-1*, *cpg-1*, *cpg-2*) in these two clusters of transcriptomes, and noticed that, with the exception of one embryo, there was a clear enrichment of germ cell genes in one of the clusters and not the other (Subramaniam & Seydoux 1999; Osborne Nishimura et al. 2015; Mello et al. 1996). We manually switched the cells from the embryo that had the opposite expression patterns as the rest of the group. We ran all the remaining transcriptomes through our gene selection (363 genes, Set 9, below) and PCA procedure. This segregated a group containing two cells of each replicate, which were enriched for expression of MSx-specific markers such as *ceh-51* (Figure 2Q; Broitman-Maduro et al. 2009). We assigned the MSx identity to these transcriptomes and reran the remaining transcriptomes through the gene selection algorithm. We performed a PCA on these remaining transcriptomes with the 224 genes selected (Set 10, below). Two cells from each embryo segregated out into a separate group (Figure 2P). These transcriptomes showed expression of the C- and D-specific gene *pal-1* (Figure 2Q; Bowerman et al. 1997), so we assigned the identity of Cx to them. Further rounds of gene selection and PCA did not yield any further distinctions between cells (not shown). The remaining transcriptomes showed enrichment of AB-specific transcripts such as T09B4.1 (Osborne Nishimura et al. 2015), which independently supported our earlier observation that these were likely all AB descendants, based on their synchronized cell division.

Sorting and identifying transcriptomes of 8-cell stage AB-descendants stage by their expression levels of notch target genes (dark green in Figure S1)

Though the 4 AB descendants of the 8-cell stage could not be distinguished from each other based on bulk gene expression, evidence from Neves & Priess 2005 suggested that these cells would show differential expression of certain targets of notch signaling. When we looked at expression levels of these genes (namely *ref-1* and *hlh-27*), we found that two cells from each replicate had about 8-fold or higher *hlh-27* transcript abundance than the other two cells, and that

one of them was enriched for *ref-1* transcripts while all the others were not (Figure 3B). In the one case where *ref-1* was detected in two AB descendant cells instead of just one, the expression level was about twice as high in one cell than the other, and so we considered the one with higher expression to be the *ref-1* positive cell from that replicate. Based on these expression levels, we hypothesized that out of the 4 AB descendants at the 8-cell stage, one is *hlh-27* positive and *ref-1* negative, two are negative for both, and one is positive for both. We queried the intact embryo for expression patterns of these genes by smFISH (fig 3C,D), and found this to be true, with the ABa daughters (ABal and ABar) not enriched for transcripts of either gene, ABpr enriched for just just *hlh-27*, and ABpl enriched for both *hlh-27* and *ref-1*.

Identifying AB-descendants of the 16-cell stage by PCA using notch target genes (light green in Figure S1)

In order to distinguish between the AB-descendants at the 16-cell stage we performed a PCA on all of these cells. Rather than using algorithm-selected genes, we used all the notch target genes that we anticipated would be differentially enriched, based on Neves & Priess 2005. The 7 genes used were *hlh-25*, *hlh-26*, *hlh-27*, *hlh-29*, *tbx-38*, *tbx-39* and *ref-1*. Though the PCA did not show precise clusters, the transcriptomes from each embryo were arranged on the PCA plot in the same "side-ways Y" formation, with two transcriptomes from each embryo in the top left corner, two in the bottom left, two in the center, and two on the right (Figure S2D). We tentatively considered all top left pairs to be the same cell type, all center pairs to be the same cell type, and so forth. In this manner we sorted the 8 AB descendants into four groups of two, which we hypothesized were sister cells. Each of these groups broadly showed a unique combination of *hlh-27*, *ref-1* and *tbx-38* transcripts (Figure 3F). Some transcriptomes did not exactly match the patterns of the others in the group. These results may either be false negatives due to low sensitivity of scRNA-seq, or may be true negatives either due to some embryos being slightly younger than the others or due to some amount of stochasticity in gene expression. We probed the intact 15-cell stage embryo for these genes by smFISH (Figure 3G,H) and found that, as predicted, one pair of cells expressed only *tbx-38* (ABala and ABalp), one pair expressed all three (ABara and ABarp), one pair expressed only *hlh-27* (ABpla and ABplp), and one pair expressed both *hlh-27* and *ref-1* (ABpra and ABprp). This allowed us to assign identities to these cells at a resolution of cell pairs.

Using AB-descendant identities at the 8-cell stage to assign identities to AB-descendants of the 4-cell stage (blue in Figure S1)

Previously, we were able to sort the ABa/ABp cells into two separate groups based on our gene selection algorithm and PCA (Figure 2F), but without candidate genes we were unable to determine which group was composed of ABa cells and which was ABp. After we identified the descendants of these two cells (ABal/ABar and ABpl/ABpr, respectively), we used gene expression data from both the 8-cell stage and the 4-cell stage to match the parent cells with their descendants. We performed a differential expression analysis comparing ABa daughters (ABal/ABar) to ABp daughters (ABpl/ABpr), and found 1054 and 1665 genes to be enriched in each group respectively. We then performed a differential expression analysis between the ABa and ABp cells (without knowing which group was which). We found 857 genes enriched in one group, and 873 genes enriched in the other. When we compared the differentially enriched genes of the parent cells with those of the descendant cells, we saw that ABal/ABar cells shared more genes with one parent cell (which we will now call ABa) than the other (Figure S2C). Conversely, the ABpl/pr cells shared more genes with the other parent cell (which we will now call ABp) than the first (ABa).

Identifying ABal and ABar cells using two pairs of cells that show differential notch target gene expression (red in Figure S1)

In the two AB descendants at the 8-cell stage that do not have *hlh-27* or *ref-1* enrichment (the ABal and ABar cells, referred to generically as ABax), we noticed that there were *tbx-38* transcripts above the 25 RPKM threshold in two embryos (Figure 3B). In those two embryos, we detected *tbx-38* predominantly in only one cell from each of the two ABax transcriptomes, even though by the following stage *tbx-38* was expressed in descendants of both of them. This suggested to us that perhaps *tbx-38* expression arises in one of these cells before the other one. We performed smFISH on intact embryos of the 8-cell stage using *tbx-38* probes, and in one case saw expression exclusively in the ABal cell (Figure 3D). In the other embryos we saw *tbx-38* expression in both ABal and ABar. We hypothesize that *tbx-38* expression begins in the anterior at the 8-cell stage and eventually becomes detectable in other cells later. Since only two replicates showed differential expression of *tbx-38* between ABal and ABar (while *tbx-38* was

undetectable in the other cells by scRNA-seq), we performed a differential expression analysis between these two *tbx-38* positive cells (ABal) and their two sister cells (ABar). This resulted in a list of differentially expressed genes between these two groups, which we then used to perform a PCA on ABax cells from all replicates (Figure S2B). The remainder of the *tbx-38* negative cells showed very little difference from each other, but we were able to draw a line through the PCA plot that segregated one cell of each embryo from its sister, which we call ABal and ABar. The support for this distinction is admittedly not very strong, but we take this as evidence that there may not in fact be many, or even any, detectable differences between ABal and ABar cells. In that case, no matter which way we sorted cells between replicates and identified them, we would have the same result, which suggests a possible baseline for false-positive differentially expressed genes.

Genes used in Principle Component Analyses

Set 1
aakb-1, aars-1, acdh-9, B0495.7, C34G6.1, C52D10.12, chs-1, cit-1.2, cpar-1, cyp-31A2, E02H4.6, F09E5.3, F10G8.9, F13H6.3, F22D6.9, F30A10.15, F31B9.3, F31E8.4, F55A12.10, F57B10.3, ger-1, gst-16, hpr-9, ife-4, K07C5.2, mce-1, nhr-10, pcbd-1, R10H10.7, rga-1, scrm-1, sec-15, sur-5, T04A8.7, T24H10.1, ugt-28, W01A11.2, W08E12.1, Y105E8B.7, Y43F8B.2, Y57A10B.6, Y61A9LA.11, ZK909.3

Set 2
aakb-1, acl-2, AH10.2, atg-10, B0334.5, btb-4, C07H6.15, C16C10.1, C17H11.6, C18E3.3, C24H10.2, C27D9.1, C33D9.13, C33G3.6, C34C6.4, C39B5.2, C39B5.6, C45B2.6, C50D2.9, cdk-2, cdr-7, ced-8, clu-1, crn-2, D2013.3, daf-14, eat-16, EEED8.12, EEED8.15, egrh-2, eif-3.H, exoc-8, F01G4.5, F02D10.6, F10G8.9, F14F11.1, F15B10.1, F20G2.2, F22D3.6, F27B3.7, F28H1.1, F32B5.6, F33G12.7, F36D1.9, F36G3.2, F36H12.2, F39F10.3, F39H12.1, F40E10.6, F40H3.1, F42A6.6, F44B9.5, F53F1.3, F55G1.7, F57B10.3, F58E10.7, F58E6.6, F59A3.2, F59B2.2, fbxa-107, gln-1, gna-1, gst-5, H40L08.1, her-1, hlb-1, hpl-1, inx-13, K01G12.3, K02D10.1, K02D10.7, K04B12.2, K04G2.11, K07A12.7, K07E3.1, K08D10.12, lbp-9, lin-23, M02B1.2, med-2, msra-1, ncs-2, nhr-100, nhr-256, pot-1, prmt-2, puf-8, R03G5.6, rme-2, rsr-2, sdz-1, secs-1, sel-8, selb-1, sma-4, smg-5, sqrd-1, sqv-1, sqv-8, sup-26, T05C1.4, T05F1.13, T08B2.8, T08B6.5, T10B11.7, T10D4.6, T11B7.1, T11G6.2, T12A2.3, T12B3.3, T16G12.4, T17A3.2, T21B10.1, T22C8.3, T23B12.6, T24E12.11, T24H10.1, T28C6.3, tag-257, tag-52, tbx-2, tbx-32, toe-4, unc-112, vab-2, VF13D12L.3, vps-34, Y113G7B.16, Y37E3.20, Y39E4B.5, Y42A5A.5, Y43D4A.6, Y48G10A.3, Y50E8A.11, Y53F4B.4, Y54F10BM.13, Y55F3AM.5, Y56A3A.28, Y57G11C.1134, Y57G11C.34, Y5H2B.3, Y6B3B.5, Y71F9AL.12, Y75B12A.2, Y87G2A.11, Y95D11A.1, ZK1010.10, ZK154.4, ZK666.1, ZK688.7

Set 3
B0024.10, bath-28, bre-3, C09B7.2, C15F1.5, C17H11.2, C43H8.2, C54G6.1, chin-1, D1054.1, D2096.7, F01G4.5, F13B12.6, F14D2.11, F17A9.2, F32A5.9, F46B6.12, F46B6.6, F53B3.5, F55G1.7, gck-2, H12D21.7, kin-25, ldh-1, M04F3.4, mboa-7, mkk-4, pnc-1, R05F9.1, sac-1, skr-10, T09B4.5, T25B9.8, tag-175, tag-345, ttyh-1, vab-2, W04E12.2, Y25C1A.6, Y48C3A.18

Set 4

abcf-3, acl-1, acl-3, aco-2, acs-11, acs-13, apb-1, arp-11, atgp-2, B0024.13, B0035.16, B0334.15, B0361.9, B0410.3, B0412.3, B0564.2, bath-36, bath-8, bca-2, bre-4, btb-4, C01G10.10, C02F5.12, C04G6.4, C05D9.7, C06A5.6, C06C3.7, C09G5.8, C11H1.2, C13B9.2, C15B12.6, C15C8.4, C17C3.1, C17E4.11, C17H11.2, C18E3.3, C23F12.4, C24H10.2, C25G4.10, C25G4.2, C26E6.6, C29F7.3, C32E8.9, C32F10.8, C33A12.12, C33D9.13, C35B1.2, C35B1.5, C35E7.11, C35E7.3, C38D4.9, C42C1.4, C48A7.2, C48B4.10, C48B4.8, C50B8.3, C50F7.4, C50F7.6, C54G4.7, C56A3.8, C56G2.5, C56G7.3, cblc-1, cdk-5, cgef-1, chin-1, cnc-10, cnd-1, cnt-2, coh-1, coq-8, cpg-2, ctns-1, cyn-9, cyp-13B2, cyp-31A3, D1005.t1, D1007.5, D1054.1, D1069.3, D1081.9, D2030.12, daf-16, daf-4, dgk-2, dhs-11, dkf-1, E03A3.5, ears-1, EEED8.16, elo-6, elpc-2, end-1, end-3, eps-8, exc-9, F02E9.7, F02H6.4, F07H5.13, F08G2.11, F08G2.4, F09F7.4, F09F7.7, F10D7.2, F11C1.7, F12F6.8, F13C5.2, F14B4.2, F14B8.2, F14D2.15, F15B10.1, F17H10.1, F18H3.4, F19F10.1, F20C5.6, F22D3.6, F23D12.4, F23F1.9, F25H5.10, F25H5.6, F27C1.4, F28B3.4, F28D9.4, F28F8.9, F30A10.1, F30A10.15, F32A5.9, F33E2.5, F34H10.3, F35D11.4, F36G3.2, F39B2.7, F39E9.21, F39F10.3, F40G9.12, F40H3.6, F41E7.1, F41H10.4, F42G8.8, F45E12.5, F46C3.4, F46C3.7, F46F11.10, F46F11.9, F48B9.8, F52B11.2, F52H2.7, F53A3.7, F53F1.3, F53H4.4, F54D5.2, F55A11.7, F55C5.10, F56A11.5, F56B3.8, F56D1.1, F56H6.2, F57C9.7, F57G9.3, F58A6.5, F58E10.1, F58E10.7, F59A3.3, F59D12.5, fbp-1, fbxa-115, fbxa-181, fbxa-192, fbxa-95, fbxb-103, fbxb-117, fbxb-19, fbxb-2, fbxb-24, fbxb-42, fbxb-43, fbxb-47, fbxb-49, fbxb-5, fbxb-56, fbxb-57, fbxb-60, fbxb-61, fbxb-63, fbxb-66, fbxb-68, fbxb-80, fbxb-86, fbxb-95, fbxc-33, fipp-1, fis-2, flap-1, gei-14, gld-4, gln-1, gln-5, gly-10, gly-4, gos-28, gst-20, H04D03.4, H25P19.1, his-24, his-32, his-5, hlh-30, hut-1, iars-2, igcm-3, ins-37, inx-7, jun-1, K01C8.6, K01C8.7, K02F3.12, K04B12.2, K04G2.6, K05F6.12, K07A12.2, K07B1.4, K07E3.4, K08F11.7, K08F4.3, K08H2.3, K10B3.5, K10H10.2, K11B4.2, K12H4.2, K12H6.7, klp-16, lbp-9, lig-4, lin-24, lin-28, lin-39, lin-59, lpin-1, lst-4, M01E11.1, M106.8, M176.11, mac-1, max-2, mboa-7, mce-1, mdh-1, mes-1, mesp-1, mir-260, moc-2, mrpl-41, mspn-1, mtm-1, mtp-18, nac-2, ncx-3, nex-2, nfyb-1, nhr-23, nhr-40, nhr-95, nkat-3, nos-1, nrf-6, nspa-8, nud-1, obr-4, pat-12, pcp-5, pcs-1, pgl-2, pmk-1, pnk-4, pqn-68, pssy-1, puf-3, pzf-1, R02F2.4, R04E5.8, R05D11.4, R05D7.5, R05H10.5, R06F6.12, R07B7.10, R07B7.2, R09A8.2, R10D12.8, R10E4.7, R11.1, R11G1.7, R12B2.2, R148.5, R166.3, R186.3, R74.6, rab-5, rab-6.2, rap-2, rgs-10, rlbp-1, rme-1, rnh-1.2, rom-1, rpl-11.2, rps-6, sago-1, sars-2, scpl-3, sdz-1, sdz-12, sdz-20, sdz-23, sdz-31, sdz-32, sdz-38, sel-11, sel-12, selb-1, sem-2, set-10, set-20, set-23, sfxn-1.5, smg-8, soc-1, sph-1, sqrd-1, sre-13, srt-13, stc-1, sur-7, syx-3, T01C3.3, T04F8.15, T05F1.13, T05G5.9, T07E3.3, T07E3.4, T08B2.11, T09B4.8, T10C6.10, T12F5.2, T16H12.3, T20B12.1, T20F10.8, T20F5.3, T20G5.9, T21B10.1, T21B4.17, T21F4.1, T24B1.1, T26E3.11, T27E9.6, T28A11.22, T28B11.1, tag-124, tag-130, tag-189, tag-224, tag-233, tag-304, tbc-11, tbc-6, tbx-11, tbx-40, thoc-1, tlp-1, tomm-40, ttyh-1, tut-1, ubxn-2, ugtp-1, umps-1, unc-101, unc-5, unc-84, vhp-1, vps-36, vps-4, vps-45, W07E6.2, W08A12.1, W08F4.3, wdr-5.2, wht-7, wip-1, Y102A5C.6, Y105C5A.25, Y106G6A.1, Y106G6D.6, Y113G7B.28, Y116A8C.26, Y23H5B.6, Y23H5B.8, Y37E3.20, Y38H6A.4, Y39B6A.43, Y39E4B.5, Y41D4A.4, Y43F4B.7, Y45F10D.7, Y45G5AM.5, Y48A5A.3, Y48B6A.6, Y48C3A.18, Y48E1B.5, Y48E1C.4, Y48G8AL.5, Y49A3A.1, Y49A3A.4, Y4C6B.5, Y50D4A.4, Y50E8A.11, Y52B11A.10, Y52B11A.2, Y53G8AR.5, Y54E10BR.2, Y54E5B.2, Y54F10AL.1, Y54F10AR.2, Y55B1BR.3, Y55F3BL.2, Y56A3A.33, Y57G11C.1134, Y61A9LA.3, Y62E10A.6, Y65B4A.6, Y67H2A.7, Y71G12B.10, Y71H2AR.3, Y73C8B.3, Y75B12A.2, Y76B12C.4, Y77E11A.6, Y82E9BR.22, Y94H6A.12, ZK1010.10, ZK1098.3, ZK1098.4, ZK1098.7, ZK1248.15, ZK20.4, ZK228.12, ZK287.7, ZK355.2, ZK512.2, ZK616.2, ZK616.5, ZK688.7, ztf-1, ztf-27, ztf-9

Set 5
abcf-3, acdh-9, acl-1, acl-4, aco-2, aip-1, apx-1, atgp-2, atm-1, B0334.15, B0410.3, B0412.3, B0564.2, bath-4, bre-4, btb-20, C01G10.10, C02F5.12, C04B4.2, C05G5.2, C06A1.4, C06A5.8, C06G4.1, C08F8.2, C10F3.4, C11H1.2, C13B9.2, C14B1.12, C14C10.6, C15C8.4, C16A3.6, C23F12.4, C24H10.2, C25G4.2, C27D8.4, C28A5.1, C33D9.13, C34E10.11, C38D4.9, C49H3.4, C53D5.1, C56E6.9, C56G2.5, C56G7.3, cblc-1, cdk-5, cdk-8, chin-1, cka-1, clpp-1, cnd-1, cyn-1, cyn-9, cyp-31A3, D2030.12, daf-4, din-1, dkf-1, dpy-27, E03A3.5, E04F6.2, ego-2, elpc-2, elpc-4, end-1, end-3, eps-8, eya-1, F02H6.4, F07H5.13, F08G2.4, F09E5.7, F09E8.2, F09F7.4, F11C1.1, F11C1.7, F18H3.4, F19F10.1, F20C5.6, F22E5.20, F25H5.10, F25H9.2, F27D4.7, F29A7.6, F30A10.15, F32A5.9, F32A7.4, F33E2.5, F33H2.2, F34H10.3, F35D11.4, F35D11.5, F35H10.7, F35H12.4, F39B2.7, F39G3.3, F40H3.6, F42A8.3, F43C1.6, F45E12.5, F53A3.7, F53B3.5, F53F1.3, F53F10.2, F54D5.7, F55A11.8, F56B3.11, F57B10.9, fbxa-115, fbxb-19, fbxb-2, fbxb-43, fbxb-5, fbxb-56, fbxb-60, fbxb-80, fbxb-95, fncm-1, gcy-28, gla-3, gld-4, gly-4, gstk-1, H04D03.4, his-24, his-5, hke-4.1, hlh-30, hnd-1, ins-37, inx-22, inx-7, jmjc-1, jtr-1, jun-1, K04B12.2, K05F6.12, K08E3.4, K08E3.5, K10B3.5, K10C8.3, K10H10.2, K11B4.2, K12H4.2, K12H6.7, kat-1, klc-2, lam-1, lin-26, lin-28, lin-39, lir-2, M01A10.1, mboa-3, mes-1, mes-6, mlcd-1, moc-2, mrpl-41, mspn-1, mtm-1, mtx-1, nex-2, nhr-23, nhr-40, nrf-6, nxf-2, obr-1, obr-4, pars-1, pmk-1, polk-1, pot-3, pptr-1, pqn-68, pyk-1, R02F2.9, R04E5.8, R05F9.1, R05F9.9, R07B7.10, R09F10.8, R10D12.8, R10E4.7, R11H6.2, R12B2.2, rbr-2, rho-1, rpl-11.2, rps-6,

rsks-1, sago-1, sdz-1, sdz-12, sdz-23, sdz-31, sdz-32, sdz-38, sec-16, sec-22, sem-2, set-23, skr-20, sre-13, sup-26, syx-3, szy-20, T04F8.15, T05A12.4, T05G5.9, T07E3.4, T08B2.11, T08G11.4, T10C6.10, T10C6.8, T12G3.7, T16H12.3, T20F10.8, T21B10.1, T21B10.4, T25D3.2, T27A3.7, T27E9.6, T28A11.22, taf-11.3, tag-304, tag-345, tbc-11, tbc-6, tbx-40, tbx-9, tpi-1, ubxn-2, ucp-4, ugt-37, vps-33.2, vps-36, vps-4, vps-45, W02F12.4, W03G9.2, W04B5.5, W07E6.2, W09B6.4, wdr-5.2, wht-7, Y102A5C.6, Y106G6A.1, Y106G6D.6, Y106G6H.14, Y113G7B.28, Y116A8C.26, Y23H5B.8, Y37E3.20, Y37H2A.1, Y38H6A.4, Y43F4B.7, Y45F10D.7, Y45G5AM.9, Y48A5A.3, Y48G8AL.15, Y49A3A.1, Y49A3A.4, Y4C6B.5, Y50D4A.4, Y50E8A.11, Y52B11A.2, Y54E10A.12, Y54E10BR.1, Y54E5A.6, Y54F10AR.2, Y54G2A.23, Y55B1BR.3, Y56A3A.33, Y61A9LA.3, Y74C9A.3, Y75B12A.2, Y75B8A.14, Y76A2B.5, Y76B12C.4, Y77E11A.6, Y92H12BR.8, Y9C9A.13, ZK1010.10, ZK1098.3, ZK1098.4, ZK1098.7, ZK1320.7, ZK20.4, ZK512.2, ZK512.4, ZK688.7, ZK856.12, ZK973.1, ZK973.2

Set 6
abcf-3, acdh-9, acl-4, arl-1, arx-6, atgp-2, B0207.6, B0412.3, B0491.6, B0564.2, bir-2, C05C10.7, C05D11.9, C06A1.4, C08C3.4, C09E7.4, C15C8.4, C23F12.4, C24H12.4, C25A1.13, C25G4.2, C26B2.7, C29F7.3, C34E10.11, C35E7.11, C35E7.3, C37H5.13, C43H6.7, C43H8.1, C44B7.11, C49F5.6, C50F4.12, cblc-1, cdk-8, cep-1, clpp-1, coh-1, cyn-3, cyn-9, cyp-31A3, dgk-2, dhs-11, dnj-14, dom-3, E02H1.1, E04F6.2, eps-8, eri-6, eya-1, F01F1.1, F07E5.5, F07H5.13, F09F7.4, F09G2.2, F10E7.6, F11C1.7, F13C5.2, F25E5.1, F25H9.2, F27C1.4, F30A10.15, F33A8.6, F33E2.5, F34H10.3, F35D11.4, F38H4.10, F40H3.6, F44G4.3, F45E12.5, F53B1.2, F54D5.7, F55F8.3, F56D1.3, fbxb-19, fbxb-57, fbxb-61, fbxb-86, fbxc-33, gex-3, gla-3, gon-2, gpa-1, gstk-1, him-3, his-5, hlh-30, igcm-3, inx-7, jun-1, K08A2.1, K08H2.4, K11B4.2, K12H4.2, ldh-1, lin-26, lin-28, M01A10.1, M176.2, M18.8, nhr-23, nhr-40, nkat-3, nuo-5, nxf-2, obr-1, pars-1, pot-3, pyk-1, R05D11.6, R05H10.2, R10D12.8, R12B2.2, rab-8, rap-2, ric-8, rsks-1, sdz-12, sqv-7, sti-1, strd-1, syx-3, szy-20, T01E8.6, T02G5.3, T03F1.8, T05F1.13, T08B2.11, T09B4.8, T10C6.10, T10C6.8, T12G3.7, T20B12.3, T25B9.8, T25D3.2, T26H2.10, tag-253, tag-335, tbx-9, thoc-1, tpi-1, vem-1, vps-4, W02F12.4, W04B5.5, W05F2.3, W09G3.1, Y106G6D.6, Y106G6H.14, Y110A7A.15, Y24F12A.3, Y37E3.20, Y39G10AR.21, Y48G8AL.15, Y49A3A.1, Y50D4A.4, Y52B11A.2, Y54E10BR.1, Y54E5A.6, Y63D3A.4, Y66D12A.16, Y71F9B.2, Y73E7A.2, Y82E9BL.2, Y9C9A.13, zip-4, ZK1320.7, ZK20.4, ZK265.6, ZK973.2

Set 7
acl-14, acp-2, acs-22, agef-1, ags-3, agt-1, alh-13, apb-1, arl-1, asns-2, atf-5, B0035.3, B0281.6, B0304.2, B0410.3, B0491.6, B0495.5, B0546.4, bath-28, bath-36, bcat-1, btb-4, C01B12.9, C01G8.1, C02C6.3, C02F5.13, C03B1.13, C03H5.2, C04F12.5, C05C10.3, C05C8.6, C05G5.5, C06H2.6, C08C3.4, C08F1.10, C08F8.2, C10C5.3, C14B1.3, C15B12.6, C15C8.4, C16E9.2, C17E4.11, C17G1.7, C18B12.6, C18E3.9, C23F12.4, C24H12.11, C25A1.13, C26E6.12, C27C12.1, C27D6.4, C27F2.9, C29A12.1, C29F7.2, C29G2.1, C30F12.4, C30G4.4, C33A12.7, C33F10.4, C33G3.4, C33H5.17, C34D4.13, C34G6.5, C35D10.10, C36A4.10, C36B1.11, C37H5.13, C40A11.4, C43D7.10, C45G7.4, C45G9.2, C46H11.2, C47E12.2, C48B4.9, C48B6.9, C49C3.8, C49F5.6, C50C3.1, C53C7.3, C56A3.4, cct-6, CD4.7, cdc-25.2, cdc-42, cdr-6, cdr-7, ced-10, ceh-13, ceh-32, ceh-43, ceh-5, ceh-51, cey-3, ckc-1, clec-157, clec-196, clk-1, clr-1, coh-4, cpn-1, crn-6, cyn-6, D2013.3, D2096.7, daf-16, daz-1, dgk-2, dmd-6, dnj-15, dpf-5, dve-1, E04F6.2, ech-2, EEED8.14, elpc-4, end-1, eng-1, ercc-1, erv-46, ess-2, eya-1, F02E9.7, F02H6.4, F08B6.1, F08B6.3, F08H9.3, F09E5.16, F09E5.7, F09F7.6, F10D11.2, F11A10.5, F11A10.6, F13D12.3, F13E9.11, F14B8.2, F14D2.11, F14H12.6, F17C11.4, F18A1.7, F21D5.4, F21D9.1, F22F7.7, F23A7.1, F25B4.2, F25G6.8, F25H8.2, F26F4.8, F26H9.2, F27D4.8, F30H5.4, F32A7.4, F32H2.10, F34D10.2, F34D10.3, F34H10.3, F35E2.8, F35E2.9, F35G2.2, F36H5.4, F37B12.3, F37C4.6, F37H8.5, F38B2.4, F38H4.10, F39H12.1, F40G12.4, F40G12.5, F40G9.20, F42A6.6, F42A8.3, F42F12.4, F42G8.7, F43C11.10, F43H9.3, F45E12.5, F47D12.5, F47D12.9, F52A8.5, F52C9.3, F52H2.5, F53C3.11, F53F8.7, F54C9.11, F54D12.4, F54D5.2, F55A3.5, F55B12.11, F55C9.5, F55F8.3, F55G1.6, F55G1.9, F56A8.4, F56B3.11, F56C9.3, F56D1.1, F56H1.6, F57B9.1, F58E10.1, F58E10.7, F59A1.10, fars-3, fbxa-104, fbxa-67, fbxb-100, fbxb-112, fbxb-116, fbxb-18, fbxb-36, fbxb-38, fbxb-5, fbxb-55, fbxb-69, fbxb-80, fbxb-96, fbxb-97, fbxc-26, fbxc-34, fbxc-39, fbxc-50, fbxc-57, fdps-1, fkh-8, flp-18, frm-2, ftn-2, ftr-1, fzr-1, gana-1, ggtb-1, glit-1, gln-3, glo-3, gly-20, gly-4, gob-1, gos-28, gst-12, gst-30, gst-42, gyg-2, H01M10.1, H14A12.3, ham-1, hex-5, his-6, hlh-26, hmg-12, hnd-1, hrdl-1, hrg-1, hsf-1, hst-6, iars-2, icl-1, ima-1, inx-7, jamp-1, K01D12.6, K04C1.2, K04F10.3, K07A1.10, K07E8.7, K08D10.13, K08F4.3, K08H2.3, K09E3.5, K12H4.3, lat-1, lbp-3, ldh-1, let-754, lon-2, lsl-1, lsm-8, lst-4, M01H9.3, M05D6.5, M117.7, M153.1, mboa-7, mdh-1, mdt-8, mkk-4, moc-3, mspn-1, mtss-1, mxl-1, mys-4, nars-1, ncbp-2, ncs-2, ncx-3, ngn-1, nhr-135, nhr-34, nhr-47, nhr-78, nlp-11, nlp-31, nol-9, nxf-1, oma-2, pars-2, pas-1, pct-1, pgp-2, pgs-1, pph-5, ppt-1, pqn-44, prdx-3, prx-3, puf-3, puf-5, pyk-1, pyk-2, R03A10.3, R05D7.4, R05D7.7, R05F9.1, R05H10.5, R05H11.1, R07D5.2, R10E4.9, R11D1.9, R11G1.7, R12C12.6, R148.4, rab-21, rab-6.2, ref-1, ref-2, rep-1, rig-1, rpr-1, scl-27, sdz-1, sdz-23, sdz-

36, sdz-37, sec-8, set-15, set-31, shc-2, skr-17, slt-1, smg-5, smg-7, spdl-1, spo-11, spr-2, spsb-2, sptl-1, sra-33, srh-217, srh-87, sri-20, srw-48, stim-1, sup-6, syp-2, T01H8.2, T02C1.1, T02G5.14, T04D3.1, T04G9.4, T05B11.1, T05E7.1, T05H4.5, T08B2.8, T09A5.5, T09A5.7, T10C6.8, T10E9.1, T12A2.5, T12G3.5, T12G3.6, T15H9.4, T19A6.1, T19B10.2, T19B4.3, T20D3.5, T20F10.2, T21C9.13, T22D1.11, T23B12.1, T24C12.3, T24D1.5, T25D10.4, T26C11.4, T26C11.9, T26C5.3, T27A1.2, T27F7.1, T28B8.1, T28F2.2, tag-175, tag-179, tag-307, tag-345, tag-72, tap-1, tbc-6, tbx-37, tbx-38, tir-1, toca-2, tre-1, try-1, tsfm-1, ttr-7, ttyh-1, ubc-20, ubh-1, ubh-4, uev-1, ugt-12, ugt-23, unc-101, unc-57, upb-1, uri-1, vha-18, vps-36, W02A11.1, W02B12.9, W02D9.2, W02F12.4, W05F2.3, W05H9.3, W08A12.1, W08F4.13, W09C3.4, W10D9.2, wrt-5, xol-1, Y105C5A.14, Y105C5B.9, Y106G6H.4, Y110A7A.15, Y116A8C.44, Y116A8C.7, Y11D7A.10, Y23H5B.1, Y26E6A.3, Y32B12B.2, Y37A1A.4, Y37E11B.2, Y38C1AA.1, Y38C1AA.12, Y38F2AR.9, Y39E4A.3, Y41C4A.17, Y41D4A.3, Y43D4A.6, Y47G6A.25, Y47G6A.4, Y48C3A.10, Y48E1B.3, Y48G1C.6, Y49A3A.3, Y49G5B.1, Y4C6B.5, Y50D4B.2, Y51B9A.3, Y51F10.2, Y51H7C.12, Y51H7C.7, Y54F10AL.1, Y54G11A.3, Y54G2A.50, Y55D5A.1, Y55F3AM.1, Y57A10A.16, Y59A8A.3, Y65A5A.1, Y67D2.5, Y71H2AM.24, Y73B6BL.23, Y73B6BL.29, Y73F8A.36, Y77E11A.6, Y7A9D.1, Y82E9BL.6, Y92H12BR.4, Y95B8A.8, Y97E10AM.1, ZC308.4, ZC376.4, ZC434.7, ZC449.3, ZC477.3, zip-4, ZK1010.10, ZK1058.5, ZK1128.1, ZK1236.7, ZK1320.11, ZK177.8, ZK228.12, ZK616.5, ZK669.4, ZK673.5, ZK688.3, ZK792.5, ZK973.1, ztf-16, ztf-23

Set 8
B0035.3, B0393.3, B0495.9, C01F6.9, C11D2.7, C27F2.10, C30F12.4, C35D10.13, C53D6.4, chp-1, cyn-13, daf-16, F25H8.1, F32D1.7, F47D12.9, F55A11.7, F55G1.6, F58A4.9, fbxc-50, fzr-1, gap-2, H04M03.3, hda-2, his-60, hmg-4, K02B2.3, K12H4.3, lab-1, lin-5, lin-52, lsl-1, lst-4, M110.3, M18.6, mdt-6, mrt-2, nfyc-1, ref-1, rgs-9, rla-1, rnf-1, rpl-17, rpl-24.2, rpl-7, rps-17, rps-26, ruvb-2, sac-1, sdz-37, skr-14, swan-1, T05E11.3, T12G3.5, T19B10.6, T24D1.5, T26E3.4, toca-2, tomm-22, tra-4, unc-119, unc-69, vha-18, W08F4.3, W09C5.8, Y37E3.8, Y49E10.4, Y54G9A.5, Y67H2A.10, Y73B6BL.23, ZC477.3, zip-4, ZK177.8, ZK637.14

Set 9
aat-9, abi-1, agef-1, ags-3, arl-1, arx-2, asns-2, B0001.2, B0035.3, B0281.6, B0303.4, B0303.7, B0304.2, B0410.3, B0432.13, B0491.6, B0495.5, bath-28, bath-36, btb-4, C03H5.2, C05C8.1, C09G1.5, C13C12.2, C14B1.12, C14B1.3, C14B9.2, C14F11.1, C24H12.11, C25A1.5, C25G4.2, C27C12.1, C27C12.4, C28C12.12, C29A12.1, C29G2.1, C30G4.4, C34C12.8, C34D4.13, C34G6.5, C36A4.10, C37H5.13, C41D11.5, C44C1.2, C45G7.4, C45G9.2, C47B2.2, C48B4.7, C49C3.8, C49F5.6, C53C7.3, C55A6.1, calu-1, cct-6, cdc-25.2, cdc-42, cdk-9, ced-10, ceh-32, ceh-43, ceh-51, chn-1, clec-157, clpp-1, cpf-1, csn-5, cul-5, cux-7, D2013.6, D2096.7, DC2.3, dct-1, dgk-2, dhs-22, dmd-6, dnc-6, duo-3, E04F6.2, ears-1, EEED8.2, elpc-4, ercc-1, erv-46, eya-1, F02H6.4, F07F6.4, F08B6.1, F08B6.3, F09E5.16, F10D11.2, F10D7.5, F13E9.11, F13G3.11, F14B8.2, F14D2.11, F17C11.4, F18H3.1, F21D5.8, F21D9.1, F22B8.7, F22D3.6, F25H8.2, F26A3.1, F27D4.8, F29B9.2, F30F8.1, F32D8.5, F34D10.3, F34H10.3, F35E2.8, F35G2.2, F37B12.3, F38B2.4, F39H12.1, F41G3.6, F42A6.6, F42A8.3, F42F12.3, F43C11.10, F46E10.2, F48E3.6, F52A8.5, F52C6.2, F52D10.2, F53C3.11, F53F10.2, F53F8.7, F54C9.11, F54D12.4, F54E7.8, F55A3.5, F55C9.5, F56A8.4, F56B3.11, F58E10.7, F59A3.4, F59C6.15, fbxb-100, fbxb-38, fbxb-5, fbxb-55, fbxb-80, fbxb-97, fbxc-26, fbxc-34, fbxc-39, fbxc-57, fkh-8, flp-18, fncm-1, frm-2, gly-4, gos-28, gpi-1, gst-16, ham-1, hgrs-1, hip-1, his-35, hlh-26, hnd-1, hrg-1, iars-2, ima-1, inx-12, inx-14, inx-22, K04C1.2, K07E8.7, K08D10.13, K08F4.3, K08H2.3, K09E3.5, K12H4.3, kup-1, lat-1, lbp-3, ldh-1, lgc-40, lin-24, lon-2, lsm-8, lst-4, M142.8, mboa-7, mdt-31, mett-10, moc-3, mom-1, mop-25.2, mtss-1, mtx-1, mys-4, nars-1, ncbp-2, ncs-2, ncx-3, nhr-135, nhr-47, nhr-78, nlp-11, nmt-1, nos-2, nxf-1, odr-4, pak-2, pars-2, pas-4, phf-5, pink-1, plc-4, pph-4.1, pqn-44, pqn-96, praf-3, prdx-3, pxd-1, pyk-2, R05D11.5, R05D7.4, R05F9.1, R05G9.3, R05H10.5, R07D5.2, R07E4.3, R09F10.3, R10D12.12, R10E4.9, R11D1.9, R11G1.7, R12E2.11, R53.1, rab-6.2, raga-1, rap-2, rars-2, rbg-1, ref-1, ref-2, rig-1, rom-5, rpl-22, rpl-25.1, rpr-1, scl-27, sdz-1, sdz-31, sec-3, sec-8, set-15, shc-2, slt-1, sma-4, smg-7, sor-1, spdl-1, srh-87, srw-48, sti-1, stim-1, sup-6, sym-4, T01H8.2, T02C1.1, T02G5.14, T02H6.1, T03G11.6, T04H1.2, T05B11.1, T05E7.1, T05F1.4, T07E3.4, T08B2.8, T09A5.5, T09E8.3, T10C6.8, T12A2.5, T13H5.8, T15H9.4, T16H12.4, T19B10.6, T19C3.5, T20F10.2, T26C11.4, T26C5.3, T27A1.2, T27F6.4, T27F7.1, T28A8.4, T28B8.1, tag-146, tag-175, tag-179, tag-277, tag-307, tag-345, tag-72, tap-1, tbc-6, tbx-9, tir-1, toca-2, tsp-21, ttr-7, ubh-1, ubh-4, uev-1, unc-112, vps-36, W02D9.2, W02F12.4, W03C9.5, W04B5.4, W05H9.3, W08A12.1, W10D9.2, xol-1, Y105C5A.14, Y110A2AR.1, Y11D7A.10, Y26E6A.3, Y32B12B.2, Y37A1A.4, Y37D8A.21, Y37E11B.2, Y39E4A.3, Y41C4A.17, Y41D4A.3, Y48C3A.10, Y48E1B.3, Y48G1C.6, Y49A3A.3, Y51B9A.3, Y51F10.10, Y51F10.4, Y51H7C.12, Y54F10AR.2, Y54G2A.50, Y55F3AM.1, Y57E12AL.1, Y5F2A.4, Y62F5A.12, Y67D2.5, Y73F8A.27, Y95B8A.8, Y97E10AM.1, ZC449.3, ZC477.3, ZK1010.10, ZK1128.1, ZK1236.7, ZK1307.9, ZK1320.11, ZK265.6, ZK632.11, ZK673.5, ZK682.2, ZK688.3, ZK792.5, ZK973.11, ztf-16, ztf-23, ztf-3

Set 10
arl-1, arrd-25, atf-5, B0035.3, B0281.6, B0303.7, bath-10, bath-36, btb-4, C01B12.9, C05C10.3, C05C8.6, C09E8.1, C14B1.3, C14F11.1, C18B12.6, C29A12.1, C29G2.1, C30G4.4, C34D4.13, C34E7.4, C34G6.5, C35D10.10, C37H5.13, C40A11.6, C45G9.2, C46H11.2, C48B6.9, C49C3.8, C49F5.6, C53C7.3, C55C3.5, C56A3.4, cct-6, cdc-25.2, cdc-42, ceh-32, clec-12, clk-1, cnd-1, cux-7, cyp-33A1, D1007.4, D2096.7, dmd-6, EEED8.14, EEED8.2, elpc-4, eng-1, eya-1, F07F6.4, F08B6.3, F10B5.8, F10D7.5, F11A10.6, F13H8.8, F14D2.11, F14D2.16, F14F11.1, F17C11.4, F22B8.7, F23A7.1, F25B4.2, F30F8.10, F32A5.9, F32D8.5, F34H10.3, F35E2.5, F35G2.2, F37B12.3, F38B2.4, F39H2.3, F40G12.4, F40G9.6, F42A8.3, F43C11.10, F45E10.2, F46E10.2, F52A8.5, F53C3.11, F53F8.7, F53G2.8, F54D12.4, F55A11.4, F55A3.5, F55B12.11, F55F8.3, F56A8.4, F56D1.1, F56D1.3, F56H1.6, F57B9.1, F58E10.7, F59A3.1, fbxa-149, fbxb-100, fbxb-112, fbxb-38, fbxb-5, fbxb-80, fbxb-97, fbxc-57, fkh-8, flp-10, frm-2, gst-12, gst-5, gstk-1, H01M10.1, hgrs-1, hlh-26, hnd-1, hsf-1, hst-2, ima-1, inx-7, jun-1, K03B8.11, K03B8.14, K07E8.7, K08D10.13, K08H10.9, K08H2.3, K11H12.7, K12H4.3, lbp-3, M01H9.3, mir-260, mtss-1, mtx-1, nars-1, ncs-2, ngn-1, nipa-1, nxf-1, pph-4.2, pqn-96, prdx-3, pyk-2, R02D3.1, R02F2.9, R04A9.7, R05D11.5, R05F9.1, R05H10.5, R07D5.2, R07E4.3, R07H5.9, R11D1.9, ref-1, ref-2, rig-1, sdz-31, sel-5, set-17, set-31, skr-17, skr-19, smg-9, srw-48, srx-92, srz-60, sup-6, T01H8.2, T02C1.1, T06D8.9, T07C12.12, T08B2.8, T09A5.5, T10C6.8, T12A2.5, T20D3.8, T20F10.2, T21C9.13, T22B2.2, T22B7.4, T26C11.4, T27F7.1, T28B8.1, tag-179, tag-345, tap-1, tbc-6, ttr-7, ttyh-1, uev-1, ugt-12, unc-101, W02A11.1, W02F12.4, W03C9.5, W08E12.1, W09C5.3, Y105C5A.1268, Y105C5A.14, Y11D7A.10, Y37A1A.4, Y37E11B.1, Y37E11B.2, Y39A1A.14, Y40A1A.2, Y41D4A.3, Y48C3A.10, Y48C3A.18, Y48C3A.20, Y48E1B.3, Y51B9A.3, Y55F3AM.1, Y57G11C.34, Y57G11C.43, Y67D2.5, Y73F8A.27, Y92H12BL.5, Y92H12BR.4, ZC376.4, ZC477.3, zig-4, zip-4, ZK1010.10, ZK1128.1, ZK1236.7, ZK402.6, ZK632.11, ZK688.3

Set 11
6R55.2, abce-1, abcf-3, abi-1, acl-9, aco-2, agef-1, aip-1, akt-2, amph-1, ani-2, apb-1, arl-8, arx-1, asns-2, asp-4, atf-5, atg-16.2, atg-3, atg-4.2, B0001.3, B0035.3, B0261.4, B0281.6, B0303.7, B0304.2, B0336.7, B0361.8, B0410.3, B0432.13, B0511.13, bath-28, btb-4, C04F12.1, C05C10.3, C05C8.6, C05D2.6, C05D9.7, C05G5.3, C06C6.10, C06G4.1, C06H2.6, C08A9.6, C08B6.7, C08F1.8, C09E8.1, C09G1.5, C11H1.3, C13C12.2, C14B1.12, C14B1.3, C15B12.6, C15H11.8, C16A11.4, C17H12.2, C18B12.4, C18B12.6, C24D10.6, C24H12.11, C24H12.7, C25H3.4, C26B9.1, C27C12.1, C27H6.9, C28C12.12, C29E4.13, C29G2.1, C30C11.4, C30G4.4, C30H6.8, C32D5.11, C33A12.7, C34E7.4, C35D10.6, C36A4.10, C36B1.11, C37H5.13, C40A11.4, C41H7.4, C42C1.10, C42C1.13, C43D7.8, C44C1.2, C45G9.2, C46C11.4, C46H11.2, C47G2.3, C48B6.9, C49C3.8, C49F5.6, C50B8.1, C50B8.3, C53A5.17, C53C7.3, C55C3.5, C56A3.4, calu-1, ccch-3, cct-6, cdc-25.2, cdc-26, cdc-48.3, cdk-5, cdk-9, ceh-32, ceh-41, clec-12, clpp-1, cnb-1, cnd-1, csnk-1, cutl-21, cux-7, D1005.1, D1014.4, D1081.7, D2063.3, D2085.3, D2096.7, deps-1, dhhc-1, dhs-29, dkf-2, dmd-6, dnc-6, dnj-21, dpm-1, duo-3, E01A2.1, E01G4.3, E02H1.5, E02H1.8, ears-1, EEED8.2, elc-1, epn-1, ercc-1, ero-1, erv-46, ess-2, eya-1, F07F6.4, F07H5.13, F08B6.1, F08B6.3, F08F3.6, F09E5.2, F10D11.2, F10G7.5, F11A10.7, F11C1.7, F13E6.5, F13E9.11, F13H8.8, F14D2.16, F18A1.8, F18H3.1, F19G12.t1, F21D5.8, F21D9.1, F21H12.1, F25B4.1, F25B4.2, F25H8.1, F26A3.1, F26F4.9, F27D4.8, F28B3.6, F30A10.15, F30A10.3, F30F8.10, F31C3.4, F32A5.9, F32D8.14, F33D4.5, F33E2.5, F34H10.3, F35E2.8, F35G2.2, F36G3.2, F37B12.3, F38B2.4, F39E9.20, F39E9.21, F39E9.7, F40G12.4, F40G9.6, F42F12.3, F42G8.7, F43C11.10, F43C11.6, F45E10.2, F45E12.5, F45H11.5, F48C5.1, F48E3.6, F52A8.5, F52D2.6, F52D2.7, F53A2.3, F53C3.11, F53F10.2, F53F8.7, F53G2.8, F54C9.11, F54D12.4, F54E7.8, F55A11.4, F56B3.4, F56H1.6, F56H9.2, F57B10.8, F57B9.1, F58B3.6, F58D2.4, F58D5.7, F58E10.7, F59A3.1, F59A3.4, fbxa-108, fbxa-120, fbxb-38, fbxb-5, fbxb-55, fbxb-77, fbxb-80, fbxb-97, fbxc-29, fbxc-34, fbxc-57, fkh-8, flp-10, frm-2, gck-1, glb-10, gon-2, gst-12, gst-16, gst-5, gstk-1, H24K24.2, her-1, hgrs-1, hif-1, hip-1, his-6, hlh-26, hnd-1, hrg-1, hsf-1, hsp-60, hst-2, hyl-2, ima-1, ima-2, immp-1, inft-1, jamp-1, jun-1, K02E7.12, K02F3.12, K03B8.11, K07A1.9, K07B1.7, K07F5.14, K08D10.13, K08F4.3, K08H10.9, K08H2.4, K10B3.5, K10B4.3, K10D2.7, K11D12.12, K11D12.5, K11H12.7, K12H4.2, K12H4.3, klp-12, kup-1, lat-1, lbp-3, let-49, lipl-7, M01A10.1, M01E11.2, M01H9.3, M05D6.5, mboa-3, mdh-1, mdt-31, mdt-4, memb-1, mett-10, mex-5, mex-6, mir-260, mkk-4, morc-1, mtx-1, mxl-2, mys-4, nars-1, ngn-1, nhr-32, nhr-87, nlp-47, nmt-1, nud-2, nxf-1, odr-4, pak-2, paqr-1, pars-2, pas-4, pgk-1, phb-1, phb-2, phf-5, pph-4.1, pptr-1, pptr-2, pqn-21, pqn-44, pqn-96, prmt-5, R02D5.1, R04A9.7, R05D11.5, R05H10.5, R07D5.2, R07H5.9, R11D1.9, R11G1.7, R12E2.11, R13H4.5, R74.7, rab-21, rab-6.2, raga-1, ran-4, ref-1, ref-2, rgs-10, rig-1, rom-5, rpl-25.1, rsr-2, sand-1, sars-2, scl-27, sdz-31, sec-8, sel-5, set-15, set-17, set-23, set-3, set-31, sgt-1, skpt-1, skr-19, sma-4, smg-9, snx-6, spat-2, spdl-1, spr-1, sra-33, srh-87, srh-9, srt-42, srw-48, srz-60, stam-1, stim-1, sto-1, sup-6, swd-2.2, T01G1.4, T01H8.2, T02C1.1, T02E1.2, T02G5.14, T02H6.1, T03F1.1, T03G11.6, T04F8.2, T04H1.2, T05F1.4, T07C12.12, T07C12.14, T08B2.11, T08B2.8, T09A5.5, T10B11.7, T10C6.8,

T11G6.5, T12A2.5, T12E12.1, T13C2.6, T13C5.6, T13H5.8, T16H12.4, T19C3.5, T20F10.2, T20G5.14, T21B10.4, T21C12.3, T22G5.3, T23B12.3, T24D1.5, T25D3.2, T25G3.1, T26A5.6, T26C11.4, T26C12.1, T27F6.4, T27F6.7, T27F7.1, T28A11.22, T28C6.10, taf-6.1, tag-179, tag-231, tag-232, tag-280, tag-307, tag-345, tap-1, tbc-6, tbx-39, tmbi-4, tpi-1, trap-3, try-1, ttr-7, ttyh-1, ubc-20, ubh-2, ugt-29, umps-1, unc-101, unc-112, unc-97, uri-1, vem-1, vps-26, W02D9.2, W02F12.4, W03C9.5, W09C3.4, W09G3.6, W10D9.6, wdr-23, xol-1, xpg-1, Y102E9.2, Y105C5A.1, Y105C5A.1268, Y105C5A.14, Y105E8A.1, Y106G6A.5, Y110A2AM.4, Y110A7A.15, Y116A8C.7, Y17G7B.18, Y18D10A.9, Y22D7AL.7, Y23H5A.2, Y26E6A.3, Y37D8A.2, Y37E11B.1, Y37E11B.2, Y39A1A.14, Y39A3CL.7, Y40A1A.2, Y41D4A.3, Y41D4A.6, Y43B11AL.1, Y47D3A.13, Y47G6A.13, Y47G6A.18, Y48A5A.3, Y48C3A.10, Y48C3A.20, Y48E1B.3, Y49A3A.4, Y50D7A.2, Y51B9A.2, Y51B9A.3, Y51F10.2, Y51F10.4, Y51H4A.937, Y53F4B.10, Y54E10BR.1, Y54E10BR.4, Y54E10BR.5, Y55F3AM.1, Y56A3A.31, Y57A10A.29, Y57E12AL.1, Y62F5A.12, Y63D3A.7, Y65A5A.1, Y67D2.5, Y67D8B.2, Y71F9AL.1, Y71G12B.6, Y73B6BL.30, Y73C8B.3, Y73E7A.6, Y74C10AL.2, Y82E9BR.22, Y92H12BL.5, Y92H12BR.4, Y95B8A.8, ZC262.8, ZC376.4, ZC376.7, ZC410.3, ZC434.7, ZC449.3, ZC477.3, zig-4, zip-4, ZK1010.10, ZK1098.3, ZK1127.5, ZK1128.1, ZK1236.7, ZK1307.9, ZK1320.11, ZK228.12, ZK287.7, ZK402.6, ZK512.2, ZK546.2, ZK563.5, ZK673.5, ZK682.2, ZK973.11, ztf-23, ztf-3

Supplementary References

Anders, S., Pyl, P. T., & Huber, W. (2014). HTSeq—a Python framework to work with high-throughput sequencing data. *Bioinformatics*, *31*(2), btu638–169. http://doi.org/10.1093/bioinformatics/btu638

Bowerman, B., Ingram, M. K., & Hunter, C. P. (1997). The maternal par genes and the segregation of cell fate specification activities in early Caenorhabditis elegans embryos. *Development (Cambridge, England)*, *124*(19), 3815–3826.

Gordon, A., & Hannon, G. J. (2010). FASTX Toolkit. http://hannonlab.cshl.edu/fastx_toolkit/index.html .

Kim, D., Pertea, G., Trapnell, C., Pimentel, H., & Kelley, R. (2013). TopHat2: accurate alignment of transcriptomes in the presence of insertions, deletions and gene fusions. *Genome Biology, 14*(4), http://doi.org/10.1186/gb-2013-14-4-r36

Maduro, M. F., Broitman-Maduro, G., Mengarelli, I., & Rothman, J. H. (2007). Maternal deployment of the embryonic SKN-1-->MED-1,2 cell specification pathway in C. elegans. *Developmental Biology*, *301*(2), 590–601. http://doi.org/10.1016/j.ydbio.2006.08.029

Maduro, M. F., Hill, R. J., Heid, P. J., Newman-Smith, E. D., Zhu, J., Priess, J. R., & Rothman, J. H. (2005). Genetic redundancy in endoderm specification within the genus Caenorhabditis. *Developmental Biology*, *284*(2), 509–522. http://doi.org/10.1016/j.ydbio.2005.05.016

Mello, C. C., Schubert, C., Draper, B., Zhang, W., Lobel, R., & Priess, J. R. (1996). The PIE-1 protein and germline specification in C. elegans embryos. *Nature*, *382*(6593), 710–712. http://doi.org/10.1038/382710a0

Subramaniam, K., & Seydoux, G. (1999). nos-1 and nos-2, two genes related to Drosophila nanos, regulate primordial germ cell development and survival in Caenorhabditis elegans. *Development (Cambridge, England)*, *126*(21), 4861–4871.

Zhu, J., Hill, R. J., Heid, P. J., Fukuyama, M., Sugimoto, A., Priess, J. R., & Rothman, J. H. (1997). end-1 encodes an apparent GATA factor that specifies the endoderm precursor in Caenorhabditis elegans embryos. *Genes & Development*, *11*(21), 2883–2896.